

DOI: 10.5937/IMPRC25106M

Original research article

## SYNTHESIS OF MOF@ALUMINUM SALINE SLAG COMPOSITES FOR CO<sub>2</sub> CAPTURE AS A NEW STRATEGY OF VALORIZATION OF SECONDARY ALUMINUM WASTES

Helir Muñoz<sup>#</sup>, 0000-0002-0481-5261,

Sophia Korili, 0000-0001-9086-4934,

Antonio Gil, 0000-0001-9323-5981,

INAMAT<sup>2</sup>, Universidad Pública de Navarra, Campus de Arrosadía, 31006,  
Pamplona, Spain

**ABSTRACT** – Metal-organic framework (MOF) materials combined with aluminum saline slag wastes represent a relatively novel research direction. This innovative approach not only leverages industrial waste for the development of advanced materials but also promotes a circular economy and reduces the ecological footprint of aluminum production. Furthermore, it addresses the inherent stability challenges of pure MOFs. Notably, this study is the first to propose that this industrial by-product can serve as a novel, cost-effective, and environmentally friendly modulator, enabling the selective transition between the MIL-96(Al) and MIL-110(Al) phases. For the first time, novel composites of MOFs and the saline slag waste resulting from the initial aluminum extraction in an acidic medium (RW1\*), have been developed. These composites, designated as MOF@RW1\*-n (n = 25, 50, 75), were synthesized via the in-situ preparation of the MOF on RW1\* using a hydrothermal treatment method and were subsequently evaluated as CO<sub>2</sub> adsorbents. The optimized content of RW1\* in the composite significantly affect its role as a modulator in the formation of specific crystalline structures, whether MIL-96(Al) or MIL-110(Al), leading to hybrid materials with excellent textural properties and thermal stability.

**Keywords:** Aluminum industrial waste, MOFs, CO<sub>2</sub> adsorption.

### INTRODUCTION

Scientific evidence indicates that the rapid increase in greenhouse gas emissions is already causing extreme weather events, rising sea levels, and more frequent wildfires, all of which contribute to the intensification of climate change [1]. The growing CO<sub>2</sub> emissions represent a major global environmental challenge, with sectors such as transportation, industry, and energy generation playing a significant role in this issue [1]. While technologies such as carbon capture, utilization, and storage (CCUS) have been implemented, more efficient solutions are required to meet the targets of the Paris Agreement [2]. In this context, metal–organic frameworks (MOFs) have emerged as promising materials for CO<sub>2</sub> capture and mitigation due to their structural versatility and high adsorption capacity, primarily through physical mechanisms such as van der Waals forces and electrostatic interactions [3]. Among them, aluminum-based MOFs (Al-MOFs),

<sup>#</sup> corresponding author: [helirjoseph.munoz@unavarra.es](mailto:helirjoseph.munoz@unavarra.es)

such as MIL-96 and MIL-110, stand out for their thermal stability, low cost, and efficiency in CO<sub>2</sub> capture [3]. However, their synthesis is complex and requires strictly controlled conditions. Both materials crystallize from similar precursor reactants, but their formation depends on precisely tuned conditions such as pH, temperature, and reaction time. MIL-96 typically forms at pH between 1 to 3 after 24 h incubation at 210 °C, whereas MIL-110 requires more stringent conditions, often including pH values below 0.3 or 3.5 – 4.0, along with extended reaction times of up to 72 h [3].

Interestingly, this study is the first to propose that aluminum saline slags, an industrial byproduct from the secondary aluminum processes, can serve as a novel, cost-effective, and environmentally friendly modulator in the MOF synthesis of MIL-96 and MIL-110. Saline slags pose significant environmental and economic challenges due to its composition, which includes aluminum oxides, fluxing salts (NaCl and KCl), and hazardous compounds such as aluminum nitride (AlN), which can release toxic gases upon contact with water [4].

Annually, 4 to 5 million tons of saline slags are generated worldwide, and its disposal remains a critical issue [5]. Research has demonstrated that aluminum extraction from saline slags using acidic solutions enables the synthesis of various functional materials, including perovskites [6], hexaaluminates [7], and pillared clays [8]. However, current approaches primarily focus on the aluminum fraction, overlooking the residual waste left after extraction (RW1\*).

This study explores the incorporation of this waste after aluminum acid extraction (RW1\*) in MOF synthesis, promoting a circular economy approach. The impact of RW1\* on the formation of crystalline structures was evaluated by analyzing the textural, structural, and chemical properties of the resulting materials, as well as their performance in CO<sub>2</sub> adsorption up to several temperatures and 80 kPa. In addition, MIL-96 was synthesized as a reference material to compare adsorption capacity and assess the effects of the waste on the final material properties.

## EXPERIMENTAL

### Aluminum extraction and production of saline slag residual (RW1)

Saline slag wastes (W) from *Iberica de Aleaciones Ligeras S.L. (IDALSA)* was processed for aluminum extraction using an acid-mediated method. The slag was treated with 2.0 M HCl under reflux at 100 °C for 2 h with a 1:15 g/mL waste-to-solution ratio [6]. The extracted aluminum was used for the synthesis of other functional materials [4,6]. The remaining solid residue was separated by centrifugation, dried at 60 °C, and labeled RW1.

### Washing of saline slag (RW1)

RW1 was washed with deionized water at 80 °C (1:15 g/mL ratio) to remove chloride salts. The slurry was centrifuged, repeatedly washed, and dried at 80 °C for 12 h, resulting in RW1\*. X-ray fluorescence (XRF) analysis confirmed a significant reduction in chlorine content, from 16.5% (RW1) to 0.32% (RW1\*), demonstrating successful dichlorination.

### Synthesis of MOF and MOF@RW1\*-n composites

MIL-96(Al) and MOF@RW1\*-n (n = 25, 50, 75) composites were synthesized by mixing aluminum nitrate nonahydrate ( $\text{Al}(\text{NO}_3)_3 \cdot 9\text{H}_2\text{O}$ , 12.21 mmol) and trimesic acid ( $\text{H}_3\text{BTC}$ , 3.92 mmol) in deionized water, stirring for 40 min, and heating at 220 °C for 48 h in a sealed Teflon-lined autoclave [9]. After cooling, the crystalline product was filtered, washed, dried, and activated by immersion in methanol for 5 days, followed by vacuum drying at 100 °C. The final product, MIL-96(Al), was stored for further applications.

MOF@RW1\*-n composites were synthesized via an *in-situ* method, following the same procedure but incorporating different RW1\* amounts (~25, 50, and 75 wt.%). The resulting materials were designated as: MOF@RW1\*-25, MOF@RW1\*-50, and MOF@RW1\*-75.

### RESULTS AND DISCUSSION

The X-ray diffraction (XRD) patterns (**Figure 1a**) reveal that the proportion of RW1\* slags used in the synthesis significantly affects the predominant crystalline phase. When lower RW1\* proportions (25% and 50%) are used, the MOF@RW1\*-25 and MOF@RW1\*-50 composites primarily exhibit the MIL-96(Al) phase, matching the XRD pattern of MIL-96(Al) synthesized with commercial aluminum. However, at a higher RW1\* proportion (75%), MOF@RW1\*-75 preferentially forms the metastable MIL-110(Al) phase. This phase is highly dependent on strict synthesis conditions and extremely low pH (0 – 0.3) [10], emphasizing the role of RW1\* as a modulator of crystalline structure formation. The XRD pattern of MIL-110(Al) shows characteristic peaks at  $2\theta = 4.8^\circ$  and  $8.3^\circ$  (**Figure 1a**) [3], confirming the formation of this metastable structure in MOF@RW1\*-75. These peaks are strong and narrow, indicating good crystallinity. The MIL-110(Al) structure (**Figure 1b**) consists of octameric aluminum clusters linked by trimesate (btc) ligands, where hexacoordinated aluminum cations form dimers stabilized by octahedral aluminum units. This arrangement generates uniform hexagonal channels (1.7 nm in diameter) (**Figure 1c**), which are crucial for adsorption applications. In contrast, MIL-96(Al) features a three-dimensional (3D) network formed by the connection of two-dimensional (2D) aluminum cluster networks through trinuclear clusters. These clusters consist of aluminum octahedra with  $\mu_3$ -oxo bridges, while the 2D networks are composed of infinite chains of interconnected  $\text{AlO}_4(\text{OH})_2$  and  $\text{AlO}_2(\text{OH})_3(\text{H}_2\text{O})$  units (**Figure 1d**) [10].

The thermogravimetric analysis (TGA) revealed that RW1\* exhibits high thermal stability, with minimal mass loss, mainly around 600 °C due to water desorption. In contrast, MIL-96(Al) and MOF@RW1\*-n composites showed three mass loss stages: (I) below 200 °C (adsorbed water release), (II) between 200–420 °C (crystalline water loss and hydroxide decomposition), and (III) between 420–740 °C (MOF structural collapse and BTC combustion). Composites with higher RW1\* content (MOF@RW1\*-50 and MOF@RW1\*-75) demonstrated greater thermal stability, highlighting the role of RW1\* in enhancing both crystallization and thermal resistance.

The SEM analysis shows that RW1\* (**Figure 2a**) exhibits a heterogeneous and amorphous morphology with irregular particle sizes and shapes, typical of a residual material composed of metallic and non-metallic compounds such as oxides and silicates. This composition prevents the formation of well-defined crystalline structures. In the

MOF@RW1\*-n composites, morphology evolves depending on RW1\* concentration. At low concentrations, the crystals exhibit well-defined hexagonal prismatic structures similar to MIL-96 (Figure 2b), suggesting controlled crystal growth. As the RW1\* concentration increases, the morphology becomes more heterogeneous, transitioning from hexagonal prisms to elongated hexagonal rods. At the highest RW1\* concentration, the particles adopt a needle-like structure associated with MIL-110, as observed in MOF@RW1\*-75 (Figure 2c), which forms under strongly acidic conditions. This gradual morphological shift indicates that RW1\* acts as a modulator of crystal growth, likely due to ion competition affecting nucleation. At low RW1\* concentrations, MIL-96—a thermodynamically stable phase—predominates, while higher concentrations favor MIL-110, a kinetically stable phase. These findings demonstrate that RW1\* not only alters morphology but also influences the stability and composition of the resulting crystalline phases.

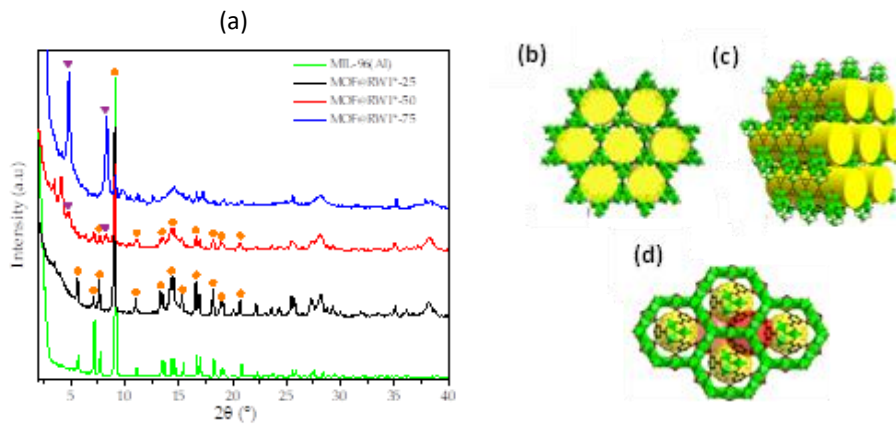


**Figure 1** XRD patterns for MIL 96(Al) and synthesized MOF@RW1\*-n composites (a). Peaks labeled with  $\blacktriangledown$ ,  $\bullet$ , represent MIL-110(Al) and MIL-96(Al), respectively. On the right, representations of MOF structures: MIL-110 (b), the 3D structure of MIL-110 showing the arrangements of the hexagonal channels (c) and MIL-96 (d) [10]

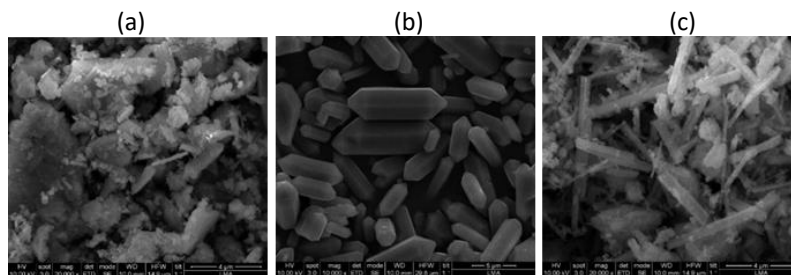


**Figure 2** SEM images for RW1\* (a), MIL-96(Al) (b), and MOF@RW1\*-75 (c)

The textural properties of aluminum saline slags (RW1 and RW1\*), MOF@RW1\*-n composites, and MIL-96(Al) were analyzed using nitrogen adsorption-desorption

isotherms at  $-196\text{ }^{\circ}\text{C}$ . Aluminum saline slags (RW1 and RW1\*) exhibited notably low BET and micropore surface areas, with values ranging from 31 to 33  $\text{m}^2/\text{g}$  and 3 to 4  $\text{m}^2/\text{g}$ , respectively, along with reduced pore volumes (0.051–0.118  $\text{cm}^3/\text{g}$ ). However, the formation of MOFs using these slags led to a marked improvement in textural properties. The synthesis method employed resulted in high BET surface areas for the prepared MOFs. As the RW1\* content increased, the BET surface area of MOF@RW1\*-n composites rose significantly, ranging from 86 to 483  $\text{m}^2/\text{g}$ . Similarly, the micropore area increased from 22 to 336  $\text{m}^2/\text{g}$ , and the total pore volume grew from 0.236 to 0.472  $\text{cm}^3/\text{g}$ . These findings suggest that the predominant formation of the MIL-110 phase contributes to improved textural properties, likely due to enhanced pore accessibility and a more open structure (**Figures 1b, c**).

When comparing the textural properties of MOF@RW1\*-75 with MIL-96(Al), a decrease in BET surface area (483 vs. 689  $\text{m}^2/\text{g}$ ) and micropore area (336 vs. 649  $\text{m}^2/\text{g}$ ) is observed. This reduction may be attributed to the incorporation of RW1\*, which decreases the proportion of micropores in the structure. However, MOF@RW1\*-75 exhibits a significantly larger total pore volume (0.472 vs. 0.264  $\text{cm}^3/\text{g}$ ), suggesting a possible reorganization of the porous structure towards larger mesopores, partially compensating for the loss of micropores.

The  $\text{N}_2$  adsorption-desorption isotherms indicate that RW1\* has a moderate adsorption capacity, corresponding to an incipient mesoporous structure with limited surface area. In contrast, the formation of MOF@RW1\*-n composites results in a shift towards a hybrid type I/IV isotherm, reflecting the coexistence of micropores from the MOF framework and mesopores from interparticle voids. Notably, MOF@RW1\*-50 and MOF@RW1\*-75 exhibit a significant increase in  $\text{N}_2$  adsorption at low relative pressures, confirming enhanced microporosity. The pore size distribution reveals mesopores ranging from 2 to 30 nm, supporting the hierarchical structure formed by integrating RW1\* into the MOF matrix. Meanwhile, MIL-96(Al) displays a classic type I isotherm, indicating its purely microporous nature, with a higher adsorption capacity compared to the composites due to its greater specific surface area.

The XPS analysis of MOF@RW1\*-50, MOF@RW1\*-75, and MIL-96(Al) confirmed the presence of Al 2p, C 1s, and O 1s peaks, along with an additional Si 2p signal in the MOF@RW1\*-50 and MOF@RW1\*-75 composites, indicating the incorporation of silicon from RW1\*. The C 1s spectrum revealed functional groups (-COOH and C-O) involved in the coordination of the organic ligand with  $\text{Al}^{3+}$ , promoting the formation of MIL-96 and MIL-110 structures. The O 1s spectrum confirmed the presence of O-Al-O bonds, characteristic of MOF frameworks, while the Al 2p peak at 73.9 eV validated the stable coordination of  $\text{Al}^{3+}$  with the ligand. These findings confirm the successful incorporation of RW1\* and the formation of stable three-dimensional MOF networks.

The EDX analysis of MOF@RW1\*-75 and MOF@RW1\*-50 confirmed the presence of aluminum (Al), oxygen (O), silicon (Si), and carbon (C), consistent with previous XPS findings. This composition verifies the successful incorporation of RW1\* into the MOF structure. Elemental mapping revealed a uniform distribution of Al and O, suggesting homogeneous integration of RW1\* and MOF precursors during synthesis. These results

confirm the effective functionalization of the materials, ensuring their structural and functional stability.

A static volumetric method is used to evaluate the CO<sub>2</sub> adsorption capacity at several temperatures [2,11]. Firstly, if the adsorption capacity of MIL-96(Al) is compared with that of other commercial MOFs (MIL-56(Al), Cu-BTC, Fe-BTC, ZIF-8 and UiO-66), a value of 1.66 mmol<sub>CO2</sub>/g is obtained compared to values between 1.03 (MIL-56(Al)) and 0.37 (ZIF-8) mmol<sub>CO2</sub>/g, all these values determined at 50 °C. In the case of MOF@waste composites, the capacities vary between 2.40 10<sup>-3</sup> mmol<sub>CO2</sub>/m<sup>2</sup> (MIL-96(Al)) and 1.95 10<sup>-3</sup> mmol<sub>CO2</sub>/m<sup>2</sup> (MOF@RW1\*-75), respectively.

## CONCLUSION

In this study, MOF@RW1\*-n composites were synthesized for the first time using a simple and cost-effective in-situ hydrothermal method. These materials were obtained from saline slags (RW1\*), a byproduct of aluminum extraction in an acidic medium. X-ray diffraction (XRD) analysis revealed that MOF@RW1\*-75 preferentially formed the metastable MIL-110(Al) phase. Furthermore, N<sub>2</sub> adsorption-desorption experiments at low pressure demonstrated that MOF@RW1\*-75 exhibited superior properties compared to MOF@RW1\*-25, MOF@RW1\*-50, and RW1\*, including a higher specific surface area, microporous surface area, and total pore volume. Scanning electron microscopy (SEM) analysis confirmed that MOF@RW1\*-75 displayed an elongated, needle-like hexagonal morphology, characteristic of the MIL-110(Al) structure. X-ray photoelectron spectroscopy (XPS) results verified the successful coordination of the ligand to the Al<sup>3+</sup> center, leading to the formation of stable three-dimensional MOF networks. Additionally, composites with a higher RW1\* content exhibited enhanced thermal stability, likely due to the intrinsic thermal resistance provided by RW1\*. These findings suggest that aluminum saline slags can serve as a precursor for synthesizing MOF composites, such as those with MIL-96(Al) and MIL-110(Al) phases, which could be effectively applied as greenhouse gas adsorbents, particularly for CO<sub>2</sub> capture at moderate temperatures between 200 and 400 °C.

## ACKNOWLEDGEMENT

*The authors are grateful for financial support from the Spanish Ministry of Science and Innovation (MCIN/AEI/10.13039/501100011033) and the Government of Navarra (Department of Rural Development and Environment, Waste Fund 2023) through projects PID2023-146935OB-C21 and 0011-4387-2023-000001. HJM thanks the Universidad Pública de Navarra for a doctoral grant.*

## REFERENCES

1. Li, P.F., Xu, Y., B. Q. (2024) *Chen, Sustain. Energy Technol. Assessments* 67, 103836.
2. Torrez-Herrera, J.J., Korili, S.A., Gil, A., (2023) *Powder Technol.* 429, 118962.
3. Haouas, M., Volkringer, C., Loiseau, T., Férey, G., Taulelle, F. (2012) *Chem. Mater.* 24, 2462–2471.
4. Muñoz, H.J., Korili, S.A., Gil, A. (2025) *Catal. Today* 447.
5. Muñoz, H.J., Korili, S.A., Gil, A. (2024) *Catal. Rev.* 00, 1–53.
6. Muñoz, H.J., Galeano, L.A., Vicente, M.A., Korili, S.A., Gil, A. (2024) *Chem. Eng. J.* 499.
7. Torrez-Herrera, J.J., Korili, S.A., Gil, A. (2022) *Chem. Eng. J.* 433, 133191.

8. Cardona, Y., Korili, S.A., Gil, A. (2021) Chem. Eng. J. 425 130708.
9. Abid, H.R., Rada, Z.H., Shang, J., Wang, S. (2016) Polyhedron 120, 103–111.
10. Li, J., Hurlock, M.J., Goncharov, V.G., Li, X., Guo, X., Zhang, Q. (2021) Inorg. Chem. 60, 4623–4632.
11. Gil, A., Arrieta, E., Vicente, M.A., Korili, S.A. (2018) Chem. Eng. J. 334, 1341–1350.